Electronic Supplementary Material (ESI) for New Journal of Chemistry.

Electronic Supplementary Information

Nanosized manganese oxide/holmium oxide: A new composite for water oxidation†

Mohammad Mahdi Najafpour,[a-c*] Saeideh Salimi,[a] Zahra Zand,[a] Małgorzata Hołyńska,[d] Tatsuya Tomo,[e] Jitendra Pal Singh[f] and Keun Hwa Chae[f] and Suleyman I. Allakhverdiev[g-i]

[a]*Department of Chemistry, Institute for Advanced Studies in Basic Sciences (IASBS), Zanjan, 45137-66731, Iran*
[b]*Center of Climate Change and Global Warming, Institute for Advanced Studies in Basic Sciences (IASBS), Zanjan, 45137-66731, Iran*
[c]*Research Center for Basic Sciences & Modern Technologies (RBST), Institute for Advanced Studies in Basic Sciences (IASBS), Zanjan 45137-66731, Iran*
[d]*Fachbereich Chemie and Wissenschaftliches Zentrum für Materialwissenschaften (WZMW), Philipps-Universität Marburg, Hans-Meerwein-Straße, D-35032 Marburg, Germany*
[e]*Department of Biology, Faculty of Science, Tokyo University of Science, Kagurazaka 1-3, Shinjuku-ku, Tokyo 162-8601, Japan*
[f]*Advanced Analysis Center, Korea Institute of Science and Technoligy, Seoul 02792, Republic of Korea*
[g]*Controlled Photobiosynthesis Laboratory, Institute of Plant Physiology, Russian Academy of Sciences, Botanicheskaya Street 35, Moscow 127276, Russia*
[h]*Institute of Basic Biological Problems, Russian Academy of Sciences, Pushchino, Moscow Region 142290, Russia*
[i]*Department of Plant Physiology, Faculty of Biology, M.V. Lomonosov Moscow State University, Leninskie Gory 1-12, Moscow 119991, Russia*
**Corresponding author; Phone: (+98) 24 3315 3201; E-mail: mmnajafpour@iasbs.ac.ir*

Water oxidation in the presence of Ce(IV)

Water oxidation experiments in the presence of Ce(IV) were performed using an HQ40d portable dissolved oxygen-meter connected to an oxygen monitor with digital readout at 25 ^{o}C. In a typical run the instrument readout was calibrated against air-saturated distilled water stirred continuously with a magnetic stirrer in an air-tight reactor. After ensuring a constant baseline reading water in the reactor was replaced with a Ce(IV) solution. Without the catalyst, Ce(IV) was stable under these conditions and oxygen evolution was not observed. After deaeration of the Ce(IV) solution with argon, catalyst as several small particles were added, and oxygen evolution was recorded with the oxygen meter under stirring (Scheme S1, ESI†). The formation of oxygen was followed and the oxygen formation rates per Mn site were obtained from linear fits of the data by the initial rate. Water oxidation was performed with the use of a setup shown in Scheme S1.

Water oxidation in the presence of $[Ru(bpy)_3]^{+3}$

Photochemical water oxidation experiments were performed in a 100 mL flask containing 80 mL of aqueous buffer (Na_2SiF_6-$NaHCO_3$, 0.028 M) with pH held at 5.8, Na_2SO_4 (300.0 mg), $Na_2S_2O_8$ (1300.0 mg), $[Ru(bpy)_3]Cl_2{\cdot}6H_2O$ (7.0 mg) and the catalyst (50.0 mg). After deaeration of the solution with Ar, the reactor was irradiated with a white LED (100 W) in a home-made device and the oxygen formation was recorded using an HQ40d portable dissolved oxygen-meter connected to an oxygen monitor with digital readout. A longpass filters (> 400 nm) from Thorlabs Company (USA) was used as a light filter.

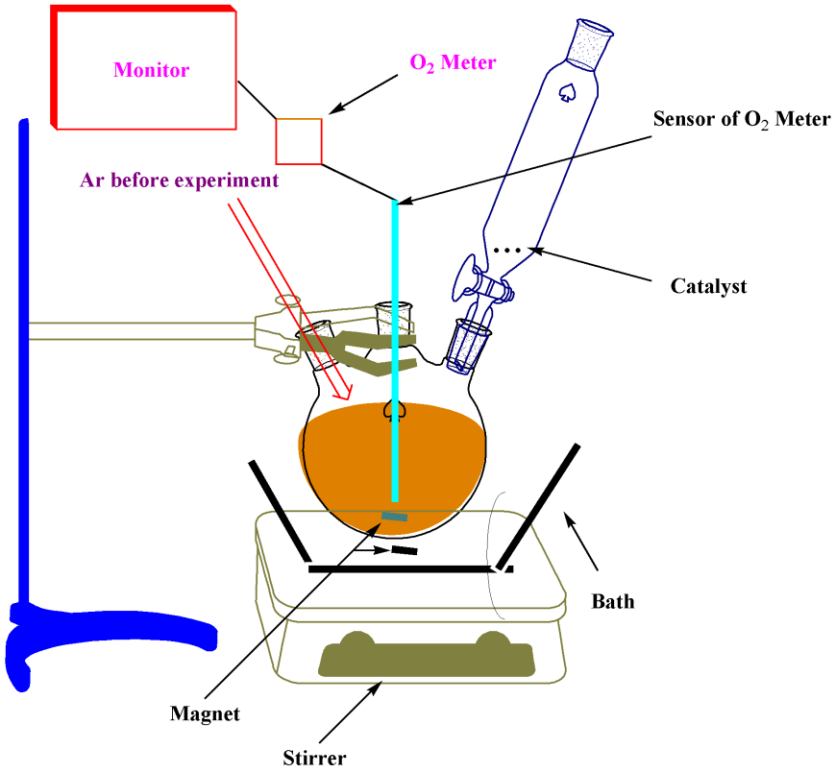

a

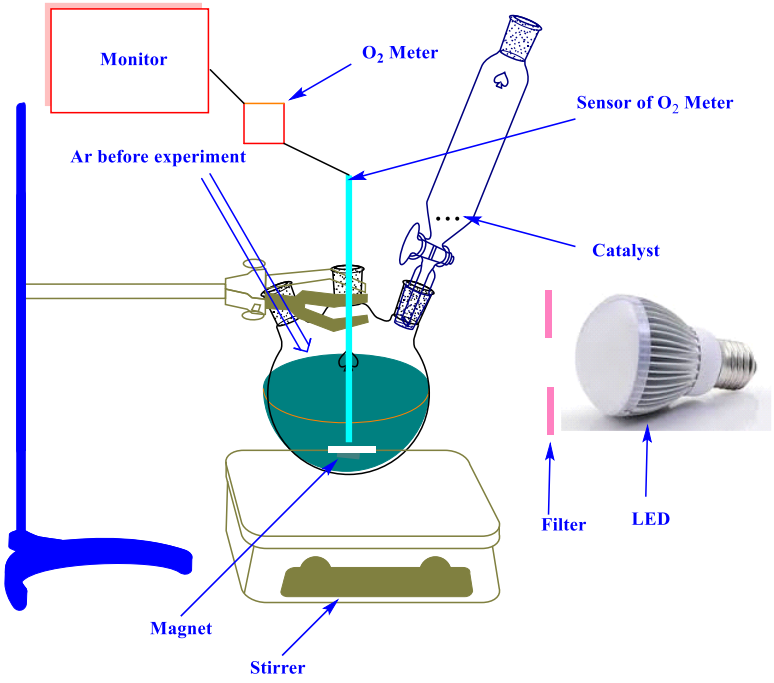

b

Scheme S1 Setup for water-oxidation reaction in the presence of Ce(IV) (a) and $Ru(bpy)_3^{3+}$ (b).

Scheme S2 Self-healing in water oxidation catalysed by Mn oxides in the presence of Ce(IV). 1: Oxygen evolution was detected with an oxygen meter. The origin of oxygen is water. 2: Mn(II) was detected by EPR. 3: The MnO_4^- ions formation could be detected with UV-Vis in a reaction of Mn(II) and Ce(IV). 4: It is known that in the reaction of Mn(II) and MnO_4^- at different pH values Mn oxide is produced. 5: The MnO_4^- ions in the presence of Mn oxide oxidize water. In this reaction, the MnO_4^- ions are reduced to Mn oxide. 6: Mn(II) in the presence of Ce(IV) forms Mn oxide. In a typical experiment, the reaction of $MnSO_4$ in the presence of Ce(IV) (1.0 M) yields MnO_2 that can be detected by XRD. Images and captions are taken ftom the ref. R1.

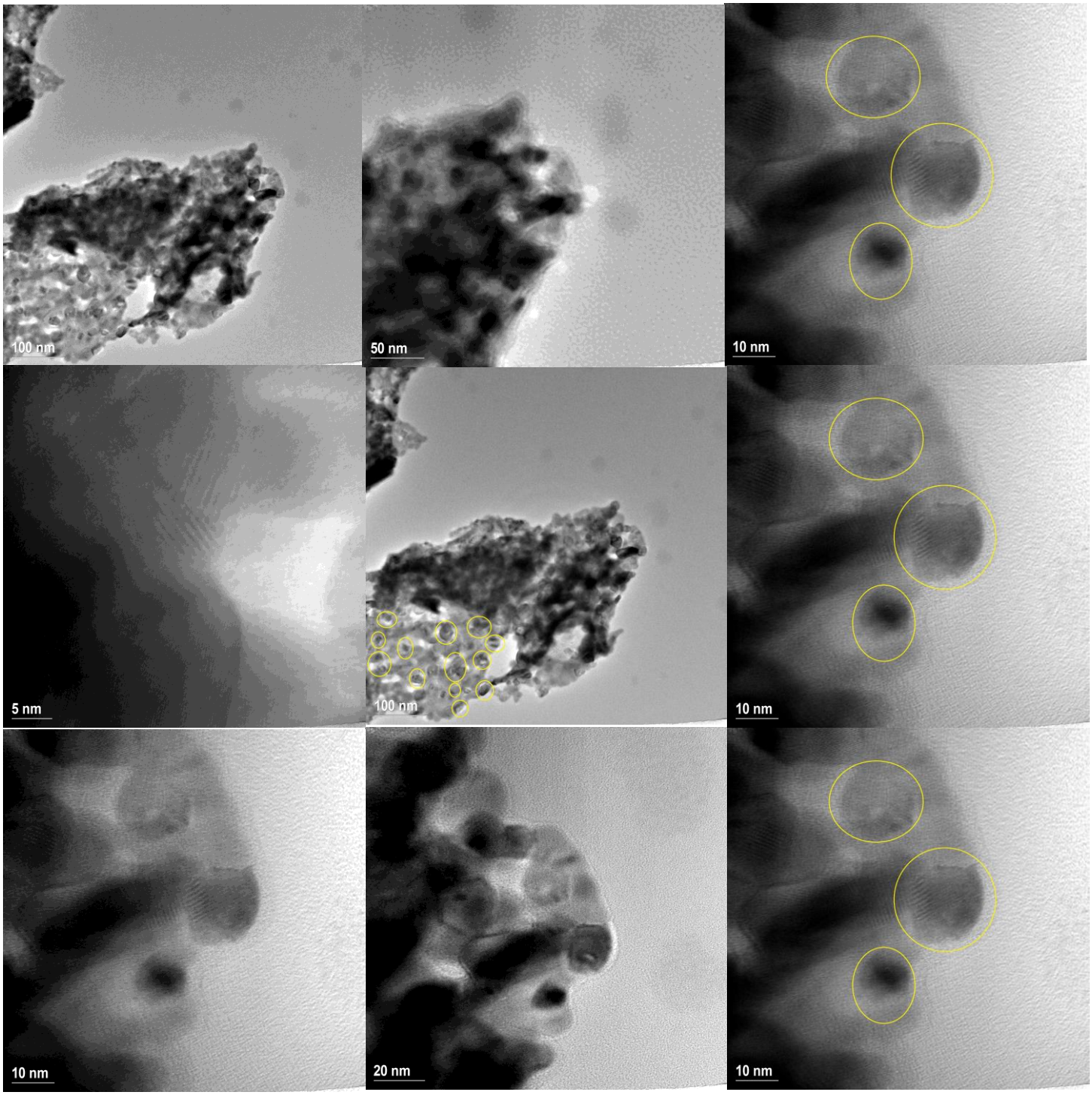

Fig. S1 TEM images for Ho_2O_3.

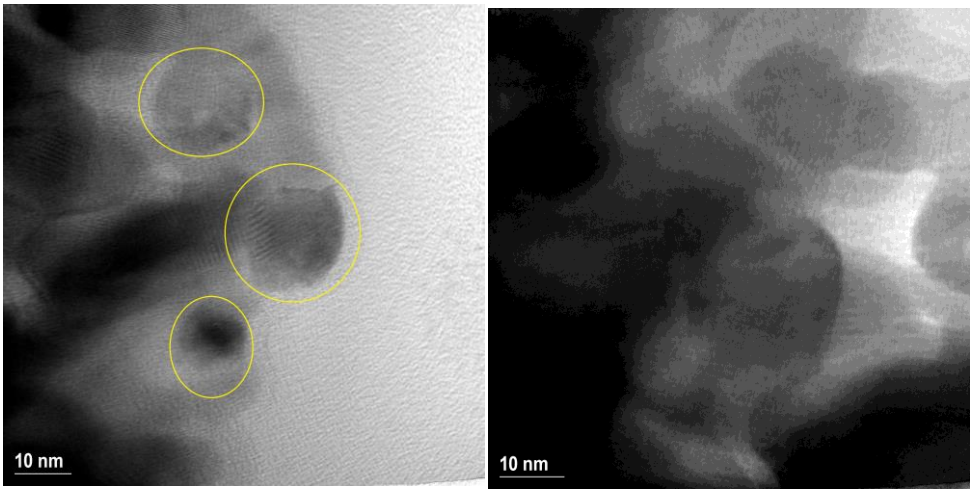

Fig. S2 TEM images for Ho_2O_3.

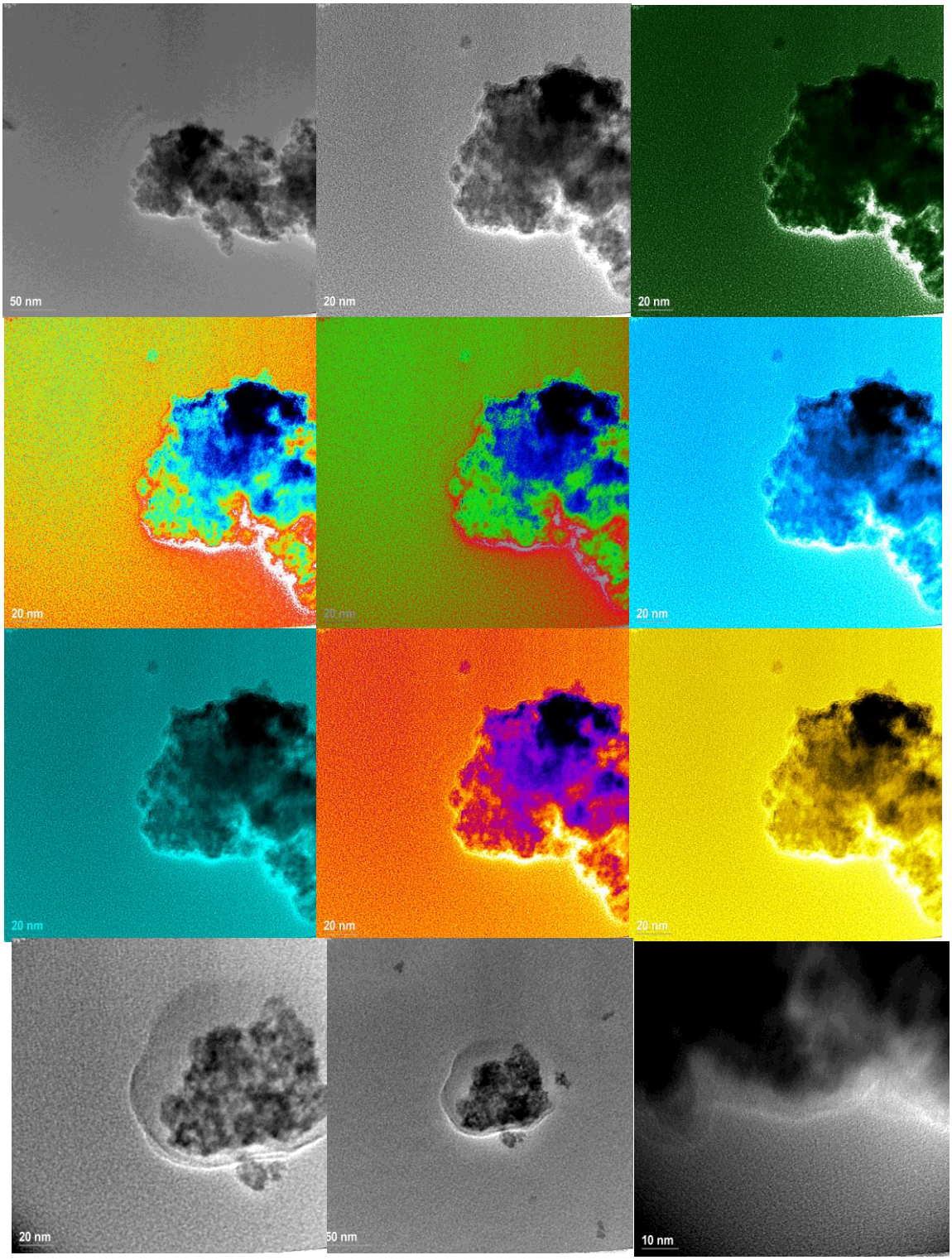

Fig. S3 TEM images for MnO_x/Ho_2O_3.

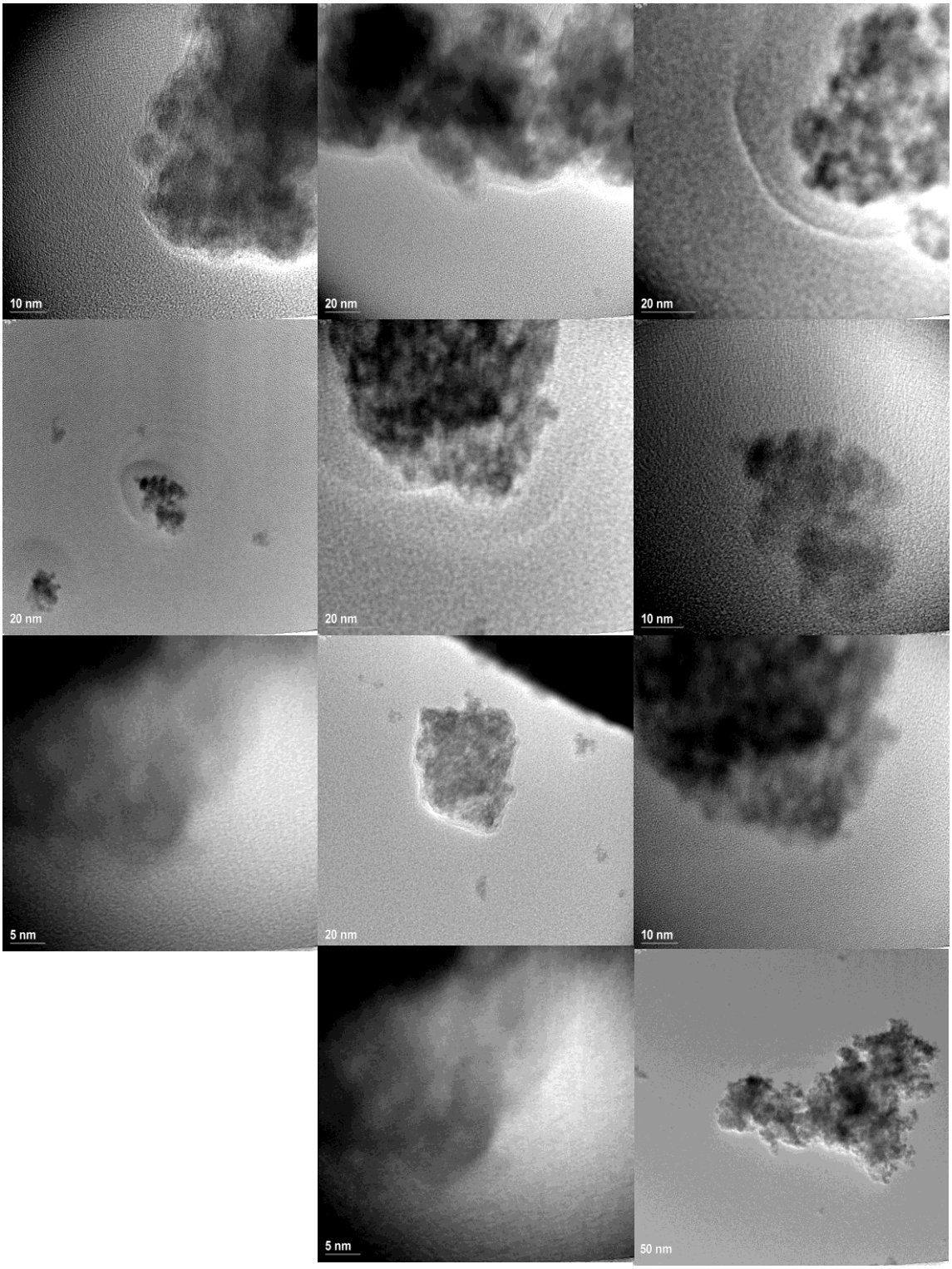

Fig. S4 TEM images for MnO_x/Ho_2O_3.

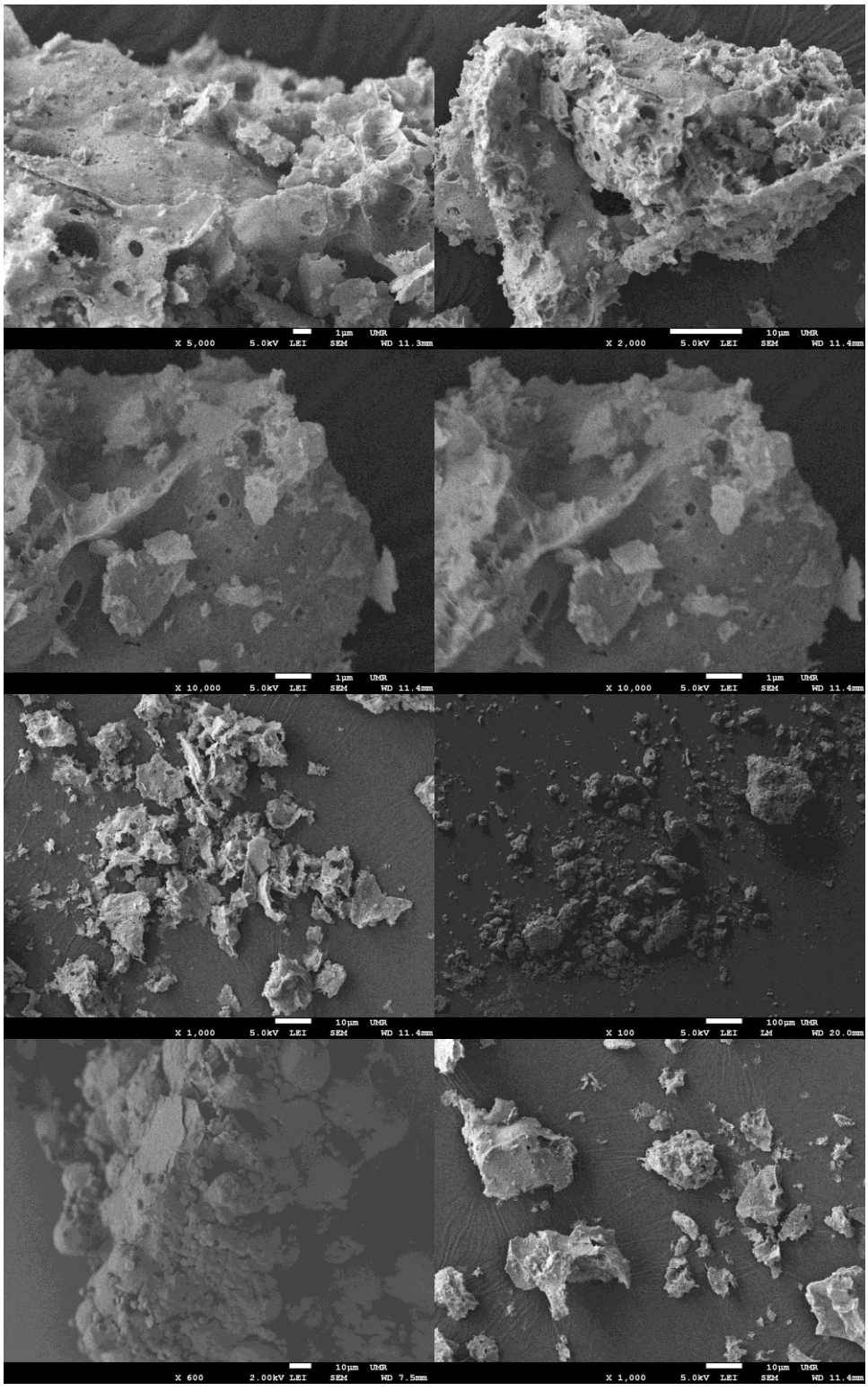

Fig. S5 SEM images for Ho_2O_3.

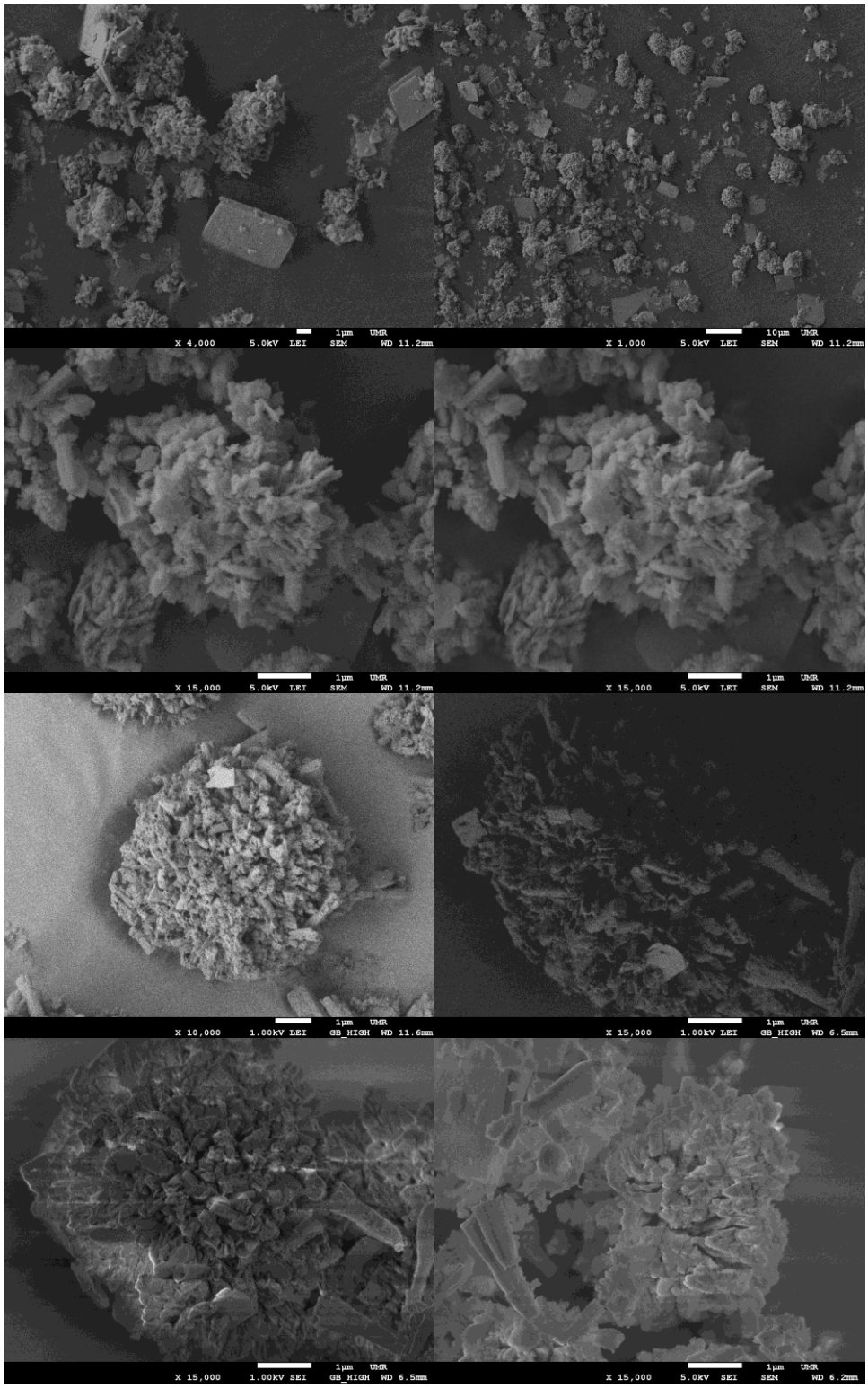

Fig. S6 SEM images for MnO_x/Ho_2O_3.

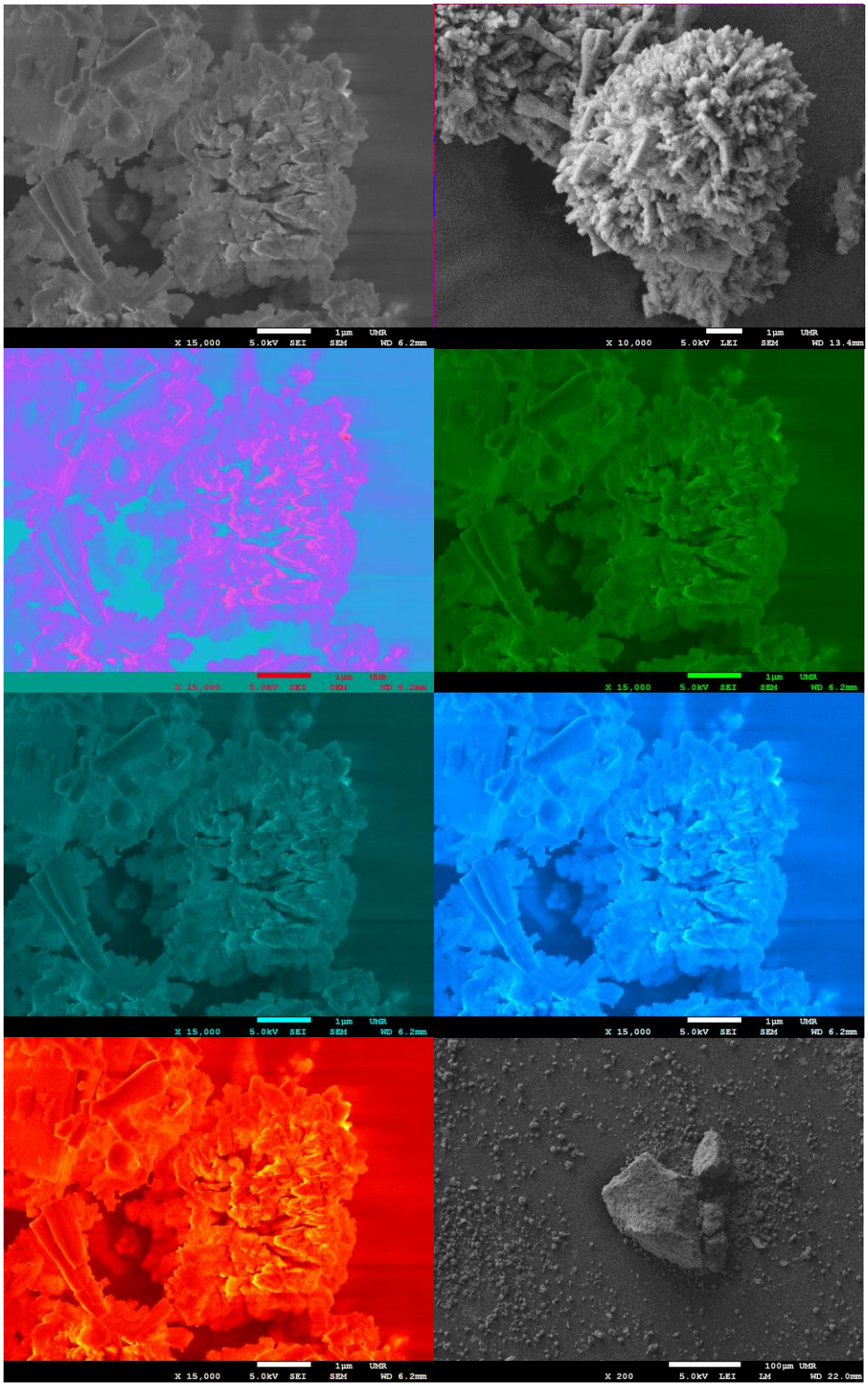

Fig. S7 SEM images for MnO_x/Ho_2O_3.

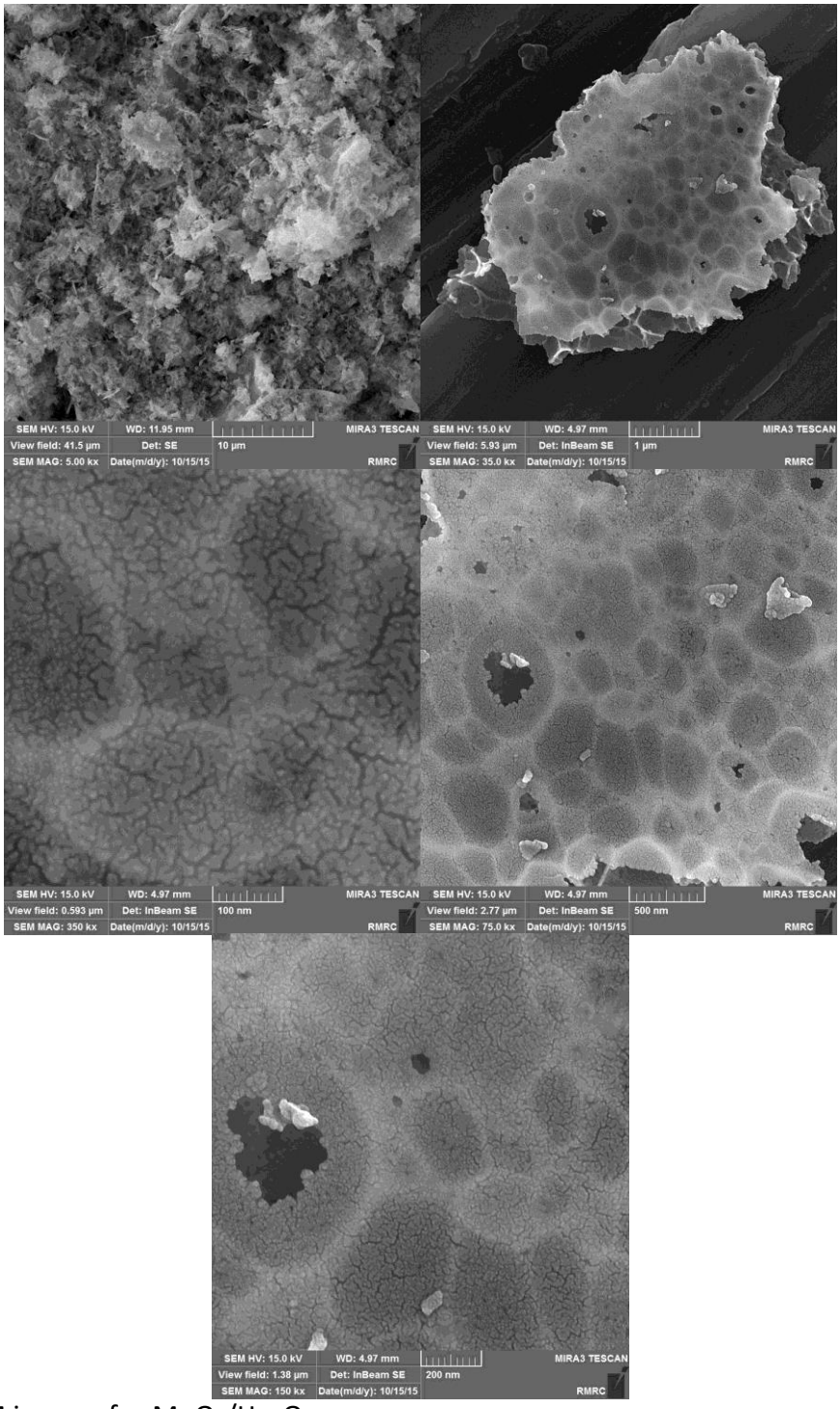

Fig. S8 SEM images for MnO_x/Ho_2O_3.

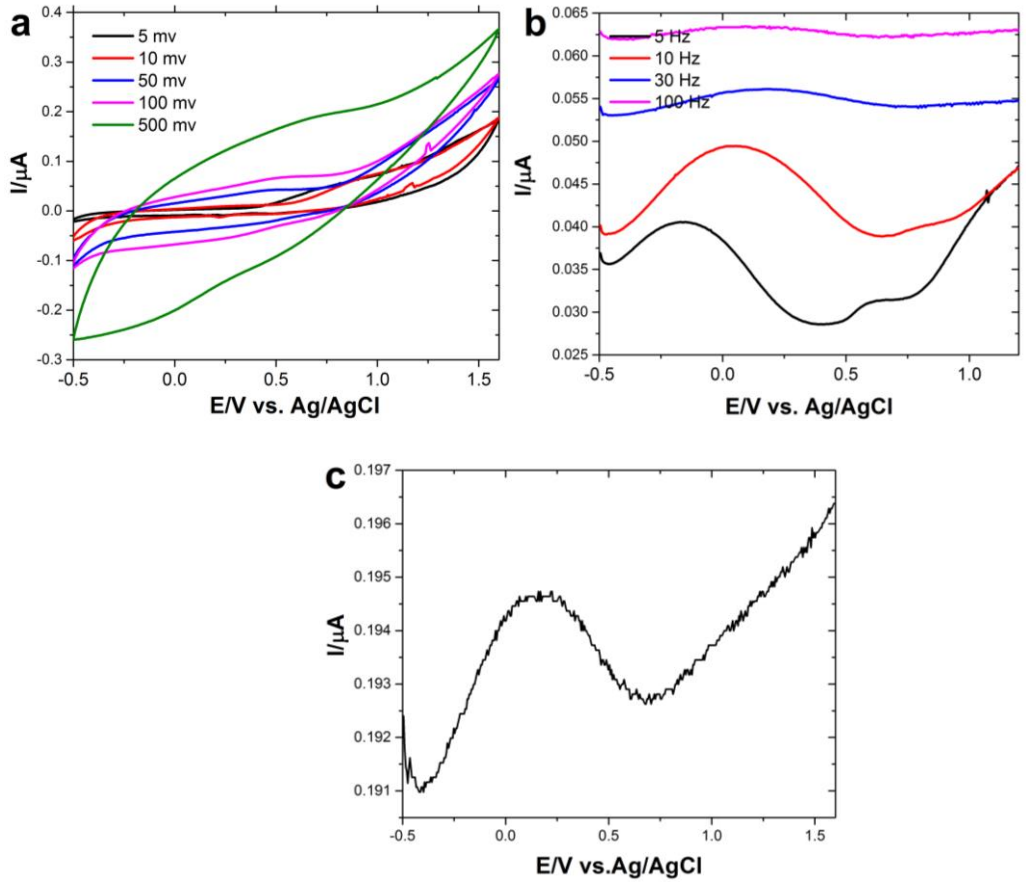

Fig. S9 CV (a), SWV at different frequencies (b) SWV at 75 mv (c) for Ho_2O_3 in $LiClO_4$ (0.25 M pH = 6.3). 30 µL of dispersed catalyst in water (1mg/mL) was dripped on the FTO and dried at room temperature. Then 10 µL of 0.5 wt % Nafion solution were cast on the surface of the FTO electrode. A three-electrode system includes FTO slide, Pt rod as counter-electrode and Ag|AgCl|KCl_{sat} as reference electrodes.

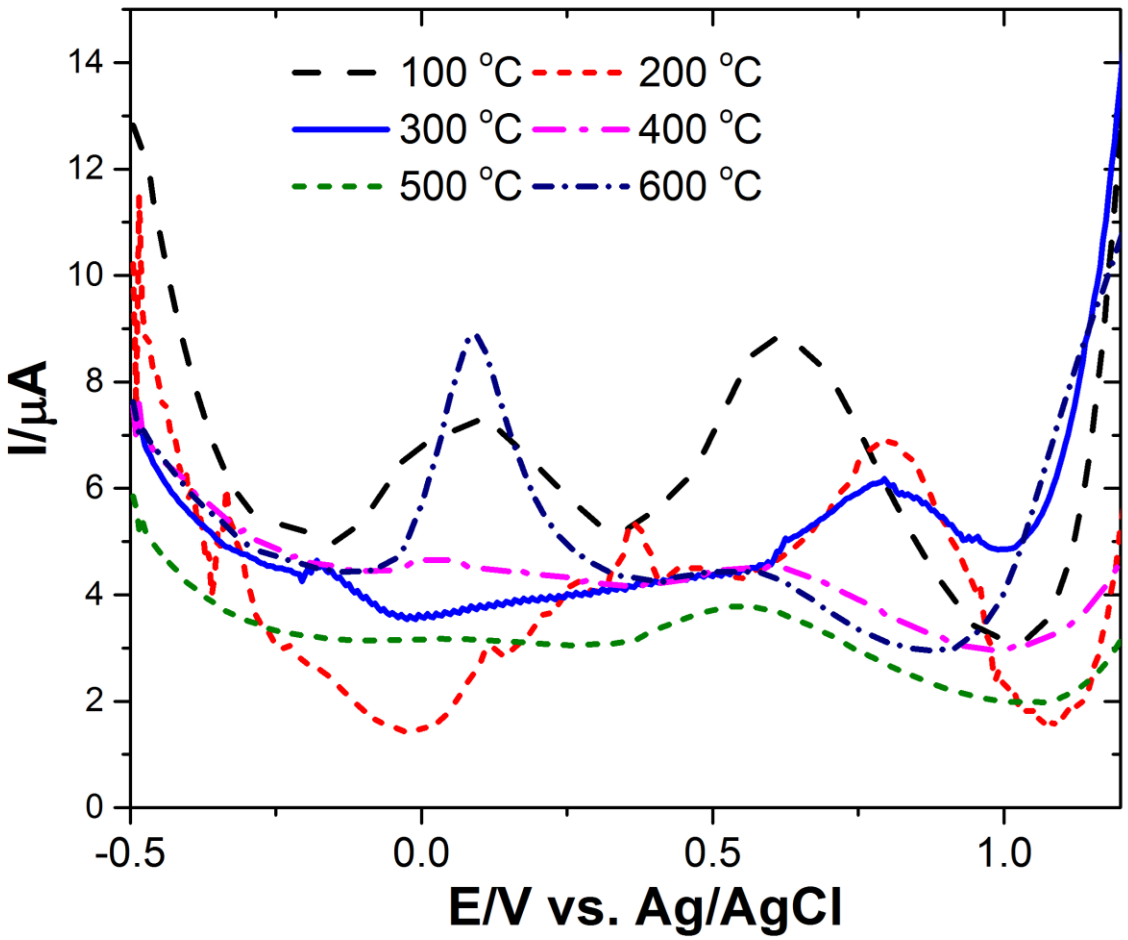

Fig. S10 SWV at 25 mv (a) for Ho_2O_3/MnO_x in different temperature. In $LiClO_4$ (0.25 M pH = 6.3). 30 µL of dispersed catalyst in water (1mg/mL) was dripped on the FTO and dried at room temperature. Then 10 µL of 0.5 wt % Nafion solution were cast on the surface of the FTO electrode. A three-electrode system includes FTO slide, Pt rod as counter-electrode and $Ag|AgCl|KCl_{sat}$ as reference electrodes.

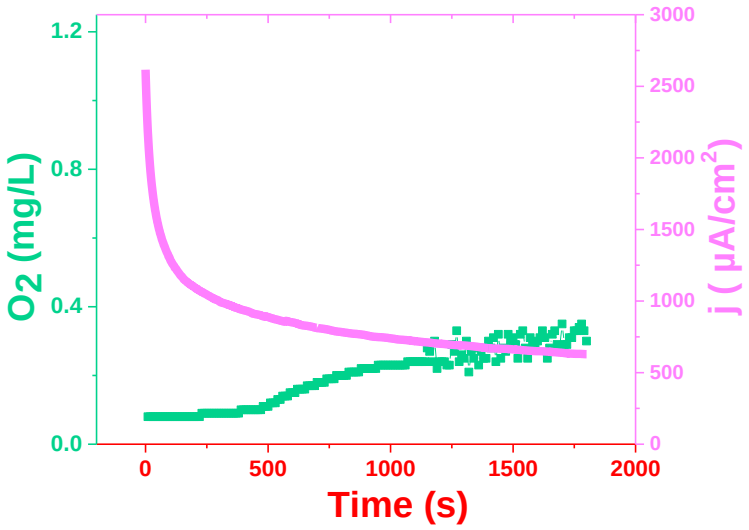

Fig. S11 Oxygen evolution/amperometry diagrams for FTO without catalyst (room temperaure, phosphate buffer (0.25 M, pH 7); 1.8 V vs. Ag|AgCl|KCl_{sat}.

Compound	Oxidant	TOF (mmol O_2/mol Mn·s)
Nanosized Mn oxide on Ho_2O_3	$Ru(bpy)_3^{3+}$ --------- Ce(IV)	0.04 ---------- 0.12
Nanosized Mn oxide on the agglomerated Silsesquioxane	Ce(IV)	0.3
Nano scale Mn oxide within NaY zeolite	Ce(IV)	2.62
Layered Mn-Ca oxide	Ce(IV)	2.2
Layered Mn-Al, Zn, K, Cd and Mg oxide	Ce(IV)	0.8-2.2
Layered Ni(II) oxide	Ce(IV)	0.4-0.6
$CaMn_2O_4.H_2O$	Ce(IV)	0.54
Amorphous Mn Oxides	$Ru(bpy)_3^{3+}$ Ce(IV)	0.06 0.52
Nano-sized Mn oxide on high surface (high surface) montmorillonite	Ce(IV)	0.5
Nanolayered Mn oxide	Ce(IV)	0.45
$CaMn_2O_4.4H_2O$	Ce(IV)	0.32
Mn oxide nanoclusters	$Ru(bpy)_3^{3+}$	0.28
β-MnO(OH)	CAN	0.24
Mn oxide-coated montmorillonite (low surface)	Ce(IV)	0.22
Layered Mn-Cu(II)	Ce(IV)	0.2-0.35
Mn_3O_4	CAN	0.01-0.17
Octahedral Molecular Sieves	$Ru(bpy)_3^{3+}$ --------- Ce(IV)	0.11 --------- 0.05
MnO_2 (colloid)	Ce(IV)	0.09
α-MnO_2 nanowires	$Ru(bpy)_3^{3+}$	0.059
$CaMn_3O_6$	Ce(IV)	0.046
$CaMn_4O_8$	Ce(IV)	0.035
Mn_2O_3	Ce(IV)	0.027
β-MnO_2 nanowires	$Ru(bpy)_3^{3+}$	0.02
$Ca_2Mn_3O_8$	Ce(IV)	0.016
$CaMnO_3$	Ce(IV)	0.012
Nano-sized λ-MnO_2	$Ru(bpy)_3^{3+}$	0.03
Bulk α-MnO_2	$Ru(bpy)_3^{3+}$	0.01
Mn Complexes	Ce(IV)	0.01-0.6
PSII	Sunlight	$100\text{-}400 \times 10^3$

Table S1 Rate of water oxidation by various Mn-based catalysts for water oxidation under the presence of non-oxo transfer oxidant. Data from R2. Turnover frequency was calculated by dividing amounts of formed oxygen, obtained by oxygen meter, by amounts of manganese, obtained by absorption spectroscopy (AAS).

Reference

R1. M. M. Najafpour, M. Khoshkam, D. J. Sedigh, A. Zahraei and M. Kompany-Zareh, *New J. Chem.*, 2015, **39.4**, 2547.
R2. M. M. Najafpour, G. Renger, M. Hołyn´ska, A. Nemati Moghaddam, E. M. Aro, R. Carpentier, H. Nishihara, J. J. Eaton-Rye, J. R. Shen and S. I. Allakhverdiev, *Chem. Rev.,* 2016, **116**, 2886.